厚生労働科学研究研究費補助金

感覚器障害研究事業

網膜血管新生抑制機構の解明とその応用に関する研究

平成１８年度　総括・分担研究報告書

主任研究者　細谷　健一

平成１９（２００７）年　３月

目　次

厚生労働科学研究費補助金（感覚器障害研究事業）
総括研究報告書

網膜ペリサイト由来新規トロポミオシンおよびシンタキシン 2D の血管内皮細胞増殖抑制機構

主任研究者　細谷　健一　富山大学・大学院医学薬学研究部　教授

研究要旨：本研究は、網膜ペリサイト由来の網膜血管内皮細胞の増殖抑制因子として同定した新規トロポミオシンおよびシンタキシン 2D の血管内皮細胞増殖抑制機構を解明することを目的とした。新規トロポミオシンは、網膜毛細血管内皮細胞株(TR-iBRB)における G1 期から S 期への移行を促進する cyclin-dependent kinase (cdk)4、cdk6 およびこれら２つの cdk と複合体を形成して細胞周期を促進する cyclin D1 の発現を減少させた。さらに DNA-polymerase-δ associated protein である proliferating cell number antigen (PCNA)の発現も減少させた。一方、シンタキシン 2D の添加においては、cdk4 の発現減少が示されたものの、他の細胞周期タンパク質には影響を与えなかった。以上の結果から、網膜ペリサイト由来新規トロポミオシンは細胞周期関連タンパク質の発現を抑制し、G1/S 期の移行を制御することで網膜血管内皮細胞の増殖抑制に関与していることが示唆された。

分担研究者　笹岡　利安　富山大学・大学院医学薬学研究部　教授

A．研究目的

糖尿病網膜症は、２大中途失明原因のひとつであり、高齢化社会を迎える日本において、失明への予防法と新たな治療薬開発が望まれている。糖尿病網膜症における血管新生は、網膜血管の周囲にあるペリサイトの脱落から始まっており、網膜ペリサイトから分泌される因子が網膜血管内皮細胞の増殖を制御していると仮説を立てた。我々が樹立した条件的不死化網膜血管内皮細胞株(TR-iBRB)と網膜ペリサイト株(TR-rPCT)の共培養解析の結果、TR-rPCT 細胞培養濃縮液を TR-iBRB 細胞に添加すると増殖が著しく抑制されることを見いだした。さらに、網膜ペリサイトから分泌される網膜血管内皮細胞の増殖抑制因子として新規トロポミオシンおよびシンタキシン 2D を同定した。本研究では、これらの２つの因子の血管内皮細胞増殖抑制機構を解明することを目的とした。

B．研究方法

網膜毛細血管内皮細胞株(TR-iBRB)および網膜ペリサイト株(TR-rPCT)は Dulbecco's modified Eagle's medium (DMEM)で培養した。TR-rPCT 細胞の conditioned medium (rPCT-CM)は TR-rPCT 細胞培養上清を限外濾過法によって濃縮した。TR-iBRB 細胞における細胞周期制御タ

ンパク質の発現変動は、Western blot 法にて解析した。

C．研究結果

rPCT-CM は TR-iBRB 細胞において、主に G1/S 期を制御しているタンパク質の発現を減少させることで細胞増殖抑制活性を示すことをすでに報告しており、新規トロポミオシンおよびシンタキシン 2D による TR-iBRB 細胞周期制御タンパク質の発現変動解析のコントロールとして用いた。TR-iBRB 細胞に、10 μM の新規トロポミオシンを添加すると rPCT-CM と同様に、G1 期から S 期への移行を促進する cyclin-dependent kinase (cdk)4、cdk6 およびこれら２つの cdk と複合体を形成して細胞周期促進する cyclin D1 の発現を減少させた。さらに DNA-polymerase-δ associated protein である(PCNA)の発現も減少させた。一方、10 μM シンタキシン 2D の添加においては、cdk4 の発現減少が示されたものの、他の細胞周期タンパク質には影響を与えなかった。TR-iBRB 細胞に導入されている SV40 large T 抗原の発現はいずれの条件下においても変化はなかった。

D．考察

TR-iBRB 細胞には細胞増殖を促進させる T 抗原遺伝子が導入されているため、増殖機構における T 抗原タンパク質の影響を考察しなければならない。Western blot 解析において、rPCT1-CM、新規トロポミオシンおよびシンタキシン 2D のいずれを添加した場合においても SV40 large T 抗原の発現量に変化は示されず、本研究における細胞増殖抑制効果に SV40 large T 抗原の影響はないことが示唆された。新規トロポミオシンおよびシンタキシン 2D は rPCT-CM 中での発現が示されていることから、本結果は新規トロポミオシンおよびシンタキシン 2D が網膜周皮細胞から内皮細胞増殖抑制因子として分泌され、ペリサイトによる網膜血管新生抑制作用の一部を担っていることを示唆している。さらに、新規トロポミオシンの増殖抑制機構は rPCT-CM と同様に網膜血管内皮細胞における細胞周期関連タンパク質の発現を抑制して G1/S 期の移行を制御することであることが示された。

E．結論

新規トロポミオシンの内皮細胞増殖抑制機構として、cyclin D1、cdk4、cdk6 の発現を減少させることで細胞周期の G1/S 期の移行を制御していることが明らかとなった。

F．健康危険情報

特になし

G．研究発表

１．論文発表

Nagase K, Tomi M, Tachikawa M, Hosoya K. Functional and molecular characterization of adenosine transport at the rat inner blood-retinal barrier. *Biochim. Biophys. Acta*, 1758, 13-19 (2006).

Katayama K, Ohshima Y, Tomi M, Hosoya K. Application of microdialysis to evaluate the efflux transport of estradiol 17-β glucuronide across the rat blood-retinal barrier. *J. Neurosci. Methods*, 156,

249-256 (2006).

Minamizono A, Tomi M, Hosoya K. Inhibition of dehydroascorbic acid transport across the rat blood-retinal and -brain barriers in experimental diabetes. *Biol. Pharm. Bull.*, 29, 2148-2150 (2006).

Nagira K, Sasaoka T, Wada T, Fukui K, Ikubo M, Hori S, Tsuneki H, Saito S, Kobayashi M. Altered subcellular distribution of estrogen receptor alpha is implicated in estradiol-induced dual regulation of insulin signaling in 3T3-L1 adipocytes. *Endocrinology*, 147, 1020-1028 (2006).

Ikesugi K, Mulhern ML, Madson CJ, Hosoya K, Terasaki T, Kador PK, Shinohara T. Induction of endoplasmic reticulum stress in retinal pericytes by glucose deprivation. *Curr. Eye Res.*, 31, 947-953 (2006).

２．学会発表

清川順平，松本悠，登美斉俊，立川正憲，近藤撤，大槻純男，寺崎哲也，細谷健一，網膜血管内皮細胞増殖に及ぼす網膜周皮細胞分泌タンパク質の影響．日本薬学会第126年会，2006年3月，仙台．

Hosoya K, Kiyokawa J, Tachikawa M, Kondo T, Ohtsuki S, Terasaki T, Tomi M, Retinal pericyte-secreted protein: Tropomyosin plays a role in suppressing retinal endothelial cell growth. Annual Meeting of the Association for Research in Vision and Ophthalmology, May 2006, Fort Lauderdale, USA.

Leal EC, Aveleira CA, Castilho A, Hosoya K, Ambrosio AF, Forrester JV, High glucose, oxidative and nitrosative stress increase leukosyte adhesion in retinal endothelial cells in culture. Annual Meeting of the Association for Research in Vision and Ophthalmology, May 2006, Fort Lauderdale USA.

Aveleira CA, Simoes NF, Fernandes CR, Meirinhos RI, Leal EC, Hosoya K, Ambrosio AF, Interleukin-1 beta type I receptor (IL-1R1) regulation in retinal endothelial cells. Annual Meeting of the Association for Research in Vision and Ophthalmology, May 2006, Fort Lauderdale, USA.

Ambrosio AF, Castilho A, Aveleira CA, Leal EC, Fernandes CR, Meirinhos RI, Simoes NF, Terasaki T, Hosoya K, Protective role of heme oxegenase-1 against high glucose and oxidative-nitorsative stress in retinal endothelial cells. May 2006, Fort Lauderdale, USA.

Kador PF, Ikesugi K, Mulhern ML, Hosoya K, Terasaki T, Blessing K, Shinohara T, Glucose imbalance induces the unfolded protein response (UPR) in rat retinal

capillary pericyte and endothelial cells. Annual Meeting of the Association for Research in Vision and Ophthalmology, May 2006, Fort Lauderdale, USA.

Makita J, Randazzo J, Blessing K, Yu K, Hosoya K, Terasaki T, Kador PF, Polyol formation in rat retinal capillary pericyte and endothelial cells. Annual Meeting of the Association for Research in Vision and Ophthalmology, May 2006, Fort Lauderdale, USA.

H. 知的財産権の出願・登録情報

1. 特許取得　なし
2. 実用新案登録　なし
3. その他　なし

厚生労働科学研究費補助金（感覚器障害研究事業）
分担研究報告書

網膜周皮細胞分泌因子による網膜血管内皮細胞増殖抑制に関わる遺伝子発現変動解析

分担研究者　立川　正憲　富山大学・大学院医学薬学研究部　助手

研究要旨：本研究は、網膜ペリサイト細胞分泌因子が網膜血管内皮細胞の遺伝子発現に及ぼす影響を網羅的に解析することで、網膜ペリサイト細胞による網膜毛細血管内皮細胞増殖抑制機構を明らかにすることを目的とした。網膜毛細血管内皮細胞株(TR-iBRB)を網膜ペリサイト株(TR-rPCT)の conditioned medium （rPCT-CM）で処理することで、plasminogen activator, urokinase、inhibitor of DNA binding 1、growth arrest and DNA-damage-inducible 45β、activating transcription factor 3 などを含む 68 遺伝子が 4 倍以上の発現変動を示し、rPCT-CM が plasminogen activator inhibitor や thrombospondin を介した血管新生の制御に関わることが示唆された。一方、TGF-βによって有意な発現変動を示した遺伝子はその一部に留まった。rPCT-CM 処理で変動を示した遺伝子は *in vivo* ラット網膜毛細血管内皮細胞において発現し、さらに虚血誘導性網膜症モデルマウスに対して rPCT-CM を投与した結果、*in vitro* と同様な網膜毛細血管内皮細胞の遺伝子の発現変動が示された。網膜ペリサイト細胞から分泌される液性因子は、細胞増殖や血管新生に関わる多数の遺伝子の発現変動を起こすことによって内皮細胞増殖抑制活性を示していることが示唆された。

A．研究目的

糖尿病網膜症は日本での成人中途失明原因の第一位となっているが、現在用いられているレーザー光や手術による治療法は網膜への侵襲が強く、治療薬の早期開発が望まれている。網膜血管内皮細胞は網膜ペリサイト細胞によって取り囲まれており、糖尿病網膜症における網膜血管新生は、網膜ペリサイト細胞が脱落することから始まる。従って、網膜ペリサイト細胞は何らかの分泌因子によって網膜血管内皮細胞の増殖を制御していると考えられているが、その詳細には不明な点が多い。そこで本研究では、網膜ペリサイト細胞分泌因子が網膜血管内皮細胞の遺伝子発現に及ぼす影響を網羅的に解析することで、網膜ペリサイト細胞による内皮細胞増殖抑制機構を明らかにすることを目的とした。

B．研究方法

網膜ペリサイト細胞および網膜血管内皮細胞の *in vitro* モデル細胞株として、それぞれ TR-rPCT 細胞、TR-iBRB 細胞を用いた。TR-rPCT 細胞培養上清（rPCT-CM）は Centriprep (Millipore) によって濃縮し

て調製した。rPCT-CM は TR-iBRB 細胞の増殖を抑えることを報告しており（*J Cell Physiol*, **203**, 378-86, (2005)）、その増殖抑制に関わる遺伝子発現変動を GeneChip (Affymetrix) を用いて解析した。さらに、リアルタイム定量 PCR 法を用いて血管新生抑制活性を持つ TGF-βによる遺伝子発現変動と比較解析した。

C．研究結果および考察

Filtering の結果、約 15000 のプローブセットの結果を 1046 のプローブセットに絞り込んだ。さらに clustering により大きく 4 つの cluster に分類した。rPCT-CM に熱処理を施すと、その細胞増殖抑制活性が消失することから、rPCT-CM の細胞増殖抑制活性特異的に変動する遺伝子が含まれると考えられる cluster I および cluster III の 934 プローブセットに着目し、これらに含まれる遺伝子を解析の主な対象とした。得られた二つの cluster に含まれる遺伝子のうち、rPCT-CM 添加によって mRNA 発現量が control の 4 倍以上に増加した遺伝子は 30 遺伝子であり、逆に control と比較して 1/4 以下に発現が減少した遺伝子は 38 遺伝子であった 。

rPCT-CM 処理で 発現が減少した遺伝子を含む cluster I には、plasminogen activator, urokinase (Plau)、annexin A3 (Anxa3)、inhibitor of DNA binding 1 (Id1) が含まれており、これらは細胞増殖または血管新生促進に関わることが報告されている。Plau は血管新生過程において基底膜の分解に関わるプロテアーゼであり、Plau とそのレセプターとの相互作用を阻害すると、網膜血管新生が抑制される。Anxa3 を細胞に過剰発現させると vascular endothelial growth factor (VEGF) の転写が促進され、AnxA3 をノックダウンした細胞では DNA 合成が阻害される。Id1 と Id3 のダブルノックアウトマウスでは腫瘍血管新生が乏しく、human umbilical vein endothelial cell (HUVEC) において Id1 および Id3 をノックダウンすると、VEGF に誘導される細胞の増殖や管腔形成が阻害されることが報告されている。

rPCT-CM により発現が増加した遺伝子を含む cluster III には、thioredoxin interacting protein (Txnip)、growth arrest and DNA-damage-inducible 45 beta (Gadd45β)、chemokine (C-X-C motif) ligand 10 (Cxcl10)、activating transcription factor 3 (Atf3) が含まれており、これらは細胞増殖抑制や血管新生抑制に関わることが報告されている。Txnip をトランスフェクトすると、細胞の成長が抑制され 、ヒト毛細血管内皮細胞において Txnip をノックダウンすると細胞の遊走が激しく誘導される。Gadd45 ファミリータンパク質は、細胞周期やアポトーシスを制御する p38 および c-jun N-terminal kinase (JNK) MAPK 経路の活性化に関与している。Cxcl10 は *in vivo* において抗血管新生効果を示し、腫瘍の進行を妨げ、レセプターとして Cxcr3 が知られている。Atf3 を内皮細胞株に発現させると、その増殖が抑制され、cyclin-dependent kinase (cdk) 2、cdk4 タンパク質の発現減少、PAI-1 mRNA の発現増加を示すことが報告されている。

GeneChip の結果から注目した遺伝子について、リアルタイム定量 PCR 法を用いて発現変動を解析した。さらに、網膜周皮細

胞に発現し、血管新生抑制活性を持つ既知のタンパク質である TGF- β1 による影響との比較解析を行った。その結果、TR-iBRB 細胞に 5X rPCT-CM を添加すると、control と比較して Plau は-7.5 倍、Anxa3 は -2.0 倍、Id1 は -3.8 倍まで有意に mRNA 発現量が減少した一方で、Txnip は 64.0 倍、Gadd45β は 8.4 倍、Cxcl10 は 19.2 倍、Atf3 は 13.0 倍まで有意に mRNA 発現量が増加しており、GeneChip の結果が反映された。また、これら 7 遺伝子うち TGF- β1 の添加においても有意な発現変動を示したものは、Plau、Id1 の 2 遺伝子にとどまり、それぞれ -3.7 倍、-3.7 倍に発現量が減少した。すなわち、本結果において rPCT-CM により示された細胞増殖関連遺伝子の発現変動は TGF-β1 のみでは説明されず、TGF-β1 が rPCT-CM の細胞増殖抑制効果の 20%程度を担うとした先の報告と一致しており、網膜周皮細胞から分泌される他の何らかの因子が更に内皮細胞増殖抑制活性に関わっていることが示唆された。また、GeneChip 解析では 4 倍以上の発現変動を示さなかったものの、血管新生の促進または抑制に関わる重要な遺伝子として知られている Id3、thrombospondin-1 (TSP-1)、plasminogen activator inhibitor type 1 (PAI-1)、Cxcr3、そして tight junction 形成に関わる occludin 遺伝子について rPCT-CM または TGF-β1 を添加した場合の時間ごと (Id3 は 48 時間のみ) の発現変動を解析した。その結果、CM の添加によって Id3 遺伝子は発現が減少し、その他の全ての遺伝子は CM を添加後 48 時間までの間に有意な発現増加を示した。このうち Id3 と PAI-1 遺伝子は TGF-β1 によっても同様の発現変動を示した。TSP-1 は抗血管新生タンパク質として知られており、網膜血管新生を抑制するほか、Gadd45β や Atf3 を介した経路により誘導されることが報告されている。PAI-1 は Plau の活性を阻害することが知られており、網膜血管新生を抑制する。

以上の結果から、rPCT1-CM は TR-iBRB 細胞において、細胞周期や基底膜分解、さらに tight junction 形成に関わる複数の経路に関わる遺伝子発現を制御し、総合的に細胞増殖を抑制している可能性が示された。

ラット網膜から網膜血管内皮細胞 (RVEC) を単離し、*in vitro* において rPCT-CM により発現が増加した遺伝子の *in vivo* での発現を解析した。その結果、解析した全ての遺伝子が RVEC に発現していることが示された。

さらに、虚血誘導性網膜症モデルマウスに対して rPCT-CM または リン酸緩衝液 (PBS) を投与した場合の RVEC における遺伝子発現変動をリアルタイム定量 PCR 法により解析した 。その結果、*in vitro* で rPCT-CM により発現が増加した遺伝子のうち、Cxcr3 を除く全ての遺伝子が rPCT-CM の投与によって PBS 投与と比較して *in vivo* 網膜血管内皮細胞においてもその発現が増加した。従って *in vitro* の結果の一部が *in vivo* においても反映され、これらの遺伝子が血管新生抑制に関わっている可能性が示された。

D. 結論

本研究によって、TR-rPCT 細胞から分泌されたタンパク質は、TR-iBRB 細胞におい

て細胞増殖促進または抑制に関わる種々の遺伝子発現を、それぞれ減少または増加させることで細胞増殖抑制活性を示していることが示唆された。*In vitro* においてrPCT-CM により発現が増加した遺伝子は、*in vivo* ラット網膜血管内皮細胞において発現していることが示された。rPCT-CM 投与による虚血誘導性網膜症モデルマウスの網膜血管新生抑制時に、*in vitro* での遺伝子発現変動の一部が *in vivo* においても反映され、それらの遺伝子が血管新生抑制に関わっている可能性が示された。

E. 健康危険情報

特になし

F. 研究発表

1. 学会発表

Hosoya K, Toki H, Tomi M, Tachikawa M, Quantitative determination of ABCA and ABCC transporter gene expression levels at the mouse inner blood-retinal barrier. AAPS Annual Meeting and Exposition, Novemver 2006, San Antonio USA.

Hosoya K., Toki H., Tomi M, Tachikawa M, ABCA and ABCC transporter mRNA expression levels at the mouse inner blood-retinal barrier. 第 21 回日本薬物動態学会年会, 2006 年 12 月, 東京.

清川 順平, 登美 斉俊, 立川 正憲, 高崎 一朗, 寺崎 哲也, 細谷 健一, 網膜血管周皮細胞分泌因子による網膜血管内皮細胞増殖抑制に関わる遺伝子発現変動解析. 日本薬学会第 127 年会, 2007 年 3 月 富山.

G. 知的財産権の出願・登録情報

1. 特許取得　なし
2. 実用新案登録　なし
3. その他　なし

研究成果の刊行に関する一覧表

発表者氏名	論文タイトル名	発表誌名	巻号	ページ	出版年
Nagase K, Tomi M, Tachikawa M, Hosoya K.	Functional and molecular characterization of adenosine transport at the rat inner blood-retinal barrier.	*Biochim. Biophys. Acta*	1758	13-19	2006
Katayama K, Ohshima Y, Tomi M, Hosoya K.	Application of microdialysis to evaluate the efflux transport of estradiol 17-β glucuronide across the rat blood-retinal barrier.	*J. Neurosci. Methods*	156	249-256	2006
Minamizono A, Tomi M, Hosoya K.	Inhibition of dehydroascorbic acid transport across the rat blood-retinal and -brain barriers in experimental diabetes.	*Biol. Pharm. Bull.*	29	2148-2150	2006
Nagira K, Sasaoka T, Wada T, Fukui K, Ikubo M, Hori S, Tsuneki H, Saito S, Kobayashi M.	Altered subcellular distribution of estrogen receptor alpha is implicated in estradiol-induced dual regulation of insulin signaling in 3T3-L1 adipocytes.	*Endocrinology*	147	1020-1028	2006
Ikesugi K, Mulhern ML, Madson CJ, Hosoya K, Terasaki T, Kador PK, Shinohara T.	Induction of endoplasmic reticulum stress in retinal pericytes by glucose deprivation.	*Curr. Eye Res.*	31	947-953	2006

Available online at www.sciencedirect.com
SCIENCE DIRECT®
Biochimica et Biophysica Acta 1758 (2006) 13–19
BIOCHIMICA ET BIOPHYSICA ACTA
BBA
http://www.elsevier.com/locate/bba

Functional and molecular characterization of adenosine transport at the rat inner blood–retinal barrier

Katsuhiko Nagase [a,b], Masatoshi Tomi [a], Masanori Tachikawa [a], Ken-ichi Hosoya [a,*]

[a] *Faculty of Pharmaceutical Sciences, University of Toyama, 2630, Sugitani, Toyama 930-0194, Japan*
[b] *Department of Hospital Pharmacy, School of Medicine, Kanazawa University, 13-1, Takara-machi, Kanazawa 920-8641, Japan*

Received 9 May 2005; received in revised form 6 December 2005; accepted 11 January 2006
Available online 2 February 2006

Abstract

The purpose of the present study was to characterize the adenosine transport system(s) at the inner blood–retinal barrier (inner BRB). A conditionally immortalized rat retinal capillary endothelial cell line (TR-iBRB2), used as an in vitro model of the inner BRB, expresses equilibrative nucleoside transporter 1 (ENT1), ENT2, concentrative nucleoside transporter 2 (CNT2), and CNT3 mRNAs. TR-iBRB2 cells exhibited an Na^+-independent and concentration-dependent [^{3}H]adenosine uptake with a Michaelis–Menten constant of 28.5 μM and a maximum uptake rate of 814 pmol/(min mg protein). [^{3}H]Adenosine uptake by TR-iBRB2 cells was strongly inhibited by 2 mM adenosine, inosine, uridine, and thymidine. On the other hand, this process was not inhibited by 100 nM nitrobenzylmercaptopurine riboside and dipyridamole. These uptake studies suggest that ENT2 is involved in [^{3}H]adenosine uptake by TR-iBRB2 cells. Quantitative real-time PCR revealed that the expression of ENT2 mRNA is 5.5-fold greater than that of ENT1 mRNA. An in vivo study suggested that [^{3}H]adenosine is transported from the blood to the retina and significantly inhibited by adenosine and thymidine. The results of this study show that ENT2 most likely mediates adenosine transport at the inner BRB and is expected to play an important role in regulating the adenosine concentration in the retina.

Keywords: Blood–retinal barrier; Adenosine; Nucleoside transporter

1. Introduction

Adenosine is an important intercellular signaling molecule and it plays a number of roles in retinal neurotransmission, blood flow, vascular development, and response to ischemia [1,2]. These effects are mediated through cell-surface adenosine receptors, so that the effect of adenosine in the retina is markedly influenced by the adenosine concentration in the retinal interstitial fluid. Most of the adenosine in the retinal interstitial fluid is thought to originate from the catabolism of adenosine monophosphate catalyzed by membrane-bound ecto-5′-nucleotidase (CD73) [1], which is localized in the innermost process of Müller cells [3]. Consequently, almost all of the retinal adenosine is distributed in the neighborhood of the innermost process of Müller cells in the ganglion cell layer, inner plexiform layer, and inner nuclear layer [4]. Retinal blood vessels are also distributed in ganglion cell layer, inner and outer plexiform layers, and inner nuclear layer [5] and form the inner blood–retinal barrier (inner BRB) which strictly regulates molecular transport between the blood and the retinal interstitial fluid [6]. Polska et al. [7] have reported that exogenous adenosine introduced via infusion increases the optic nerve head blood flow in healthy humans. Since adenosine in the blood needs to penetrate the inner BRB in order to activate its receptors expressed in vascular smooth muscle cells and increase blood flow, it has been suggested that adenosine transport system(s) at the inner BRB also have the ability to regulate the adenosine concentration in the retinal interstitial fluid and modulate retinal functions.

Two classes of nucleoside transporters have been described. The Na^+-independent equilibrative nucleoside transporter

Abbreviations: BRB, blood–retinal barrier; TR-iBRB2, conditionally immortalized rat retinal capillary endothelial cell line; NBMPR, nitrobenzylmercaptopurine riboside; ENT, equilibrative nucleoside transporter; CNT, concentrative nucleoside transporter; ECF, extracellular fluid; V_d, apparent retina-to-plasma concentration ratio; R_B, apparent blood-to-plasma concentration ratio; $K_{in,\ retina}$, apparent retinal uptake clearance of [^{3}H]adenosine; RUI, retinal uptake index; BBB, blood–brain barrier

* Corresponding author. Tel.: +81 76 434 7505; fax: +81 76 434 5172.
E-mail address: hosoyak@ms.toyama-mpu.ac.jp (K. Hosoya).

0005-2736/$ - see front matter © 2006 Elsevier B.V. All rights reserved.
doi:10.1016/j.bbamem.2006.01.011

(ENT) consists of ENT1 (Slc29a1) and ENT2 (Slc29a2) [8] while the Na^+-dependent concentrative nucleoside transporter (CNT) consists of CNT1 (Slc28a1), CNT2 (Slc28a2), and CNT3 (Slc28a3) [9]. They affect the concentration of adenosine available to its receptors in some organs. The inhibition of ENT1-mediated transport by the selective inhibitor, nitrobenzylmercaptopurine riboside (NBMPR), and consequent elevation of the adenosine concentration modulates glutamatergic synaptic transmission via presynaptic A_1 receptors in the superficial dorsal horn of the spinal cord in rats [10]. Moreover, the A_1 receptor-mediated chronotropic effect of adenosine is potentiated by the ENT1 inhibitor, dipyridamole, in the sinoatrial node of the guinea pig heart [11]. In the retina, it has been reported that [^{3}H]adenosine uptake and its inhibition by NBMPR take place in the retinal ganglion cell layer and inner nuclear layer of rabbits [12] and the cultured retinal neurons and photoreceptors of the chick embryo [13]. However, there is no information at all on the nucleoside transport system at the inner BRB although it would be very useful to have more information about adenosine transport mechanisms at the inner BRB in order to understand the regulation of the adenosine concentration in the neural retina.

The purpose of the present study was to elucidate the molecular mechanism of adenosine transport at the inner BRB. The characteristics and functions of adenosine transport at the inner BRB were examined using a conditionally immortalized rat retinal capillary endothelial cell line (TR-iBRB2) as an in vitro model of the inner BRB [14] and in vivo vascular injection techniques. TR-iBRB2 cells possess endothelial markers and glucose transporter 1 (GLUT1), P-glycoprotein, creatine transporter (CRT), and L-type amino acid transporter 1 (LAT1) [14–17], which are expressed at the inner BRB in vivo. Accordingly, TR-iBRB2 cells maintain certain in vivo functions and are a suitable in vitro model for the inner BRB.

2. Materials and methods

2.1. Animals

Male Wistar rats, weighing 250–300 g, were purchased from SLC (Shizuoka, Japan). The investigations using rats described in this report conformed to the provisions of the Animal Care Committee, Toyama Medical and Pharmaceutical University (currently University of Toyama) (#2003-48) and the ARVO Statement on the Use of Animals in Ophthalmic and Vision Research.

2.2. Cell culture

TR-iBRB2 cells were established from a transgenic rat harboring temperature-sensitive SV 40 large T-antigen gene [14]. TR-iBRB2 cells were seeded onto rat tail collagen type I-coated culture flasks (BD Biosciences, Bedford, MA). The cells were cultured in Dulbecco's modified Eagle's medium supplemented with 10% fetal bovine serum (Moregate, Bulimbra, Australia) at 33 °C in a humidified atmosphere of 5% CO_2/air. The permissive temperature for TR-iBRB2 cell culture is 33 °C due to the presence of temperature-sensitive SV40 large T-antigen [14].

2.3. RT-PCR analysis

Total cellular RNA was prepared by using an Rneasy Kit (Qiagen, Hilden, Germany). Single-strand cDNA was made from total RNA by reverse transcription (RT) using oligo dT primer. The polymerase chain reaction (PCR) was performed with ENT1 (Slc29a1), ENT2 (Slc29a2), CNT1 (Slc28a1), CNT2 (Slc28a2), or CNT3 (Slc28a3) specific primers through 40 cycles of 94 °C for 30 sec, 60–62 °C for 30 sec, and 72 °C for 1 min. The sequences of the specific primers were as follows: the sense sequence was 5′-GCC AAC TAC ACA GCC CCC ATC A-3′ and the antisense sequence was 5′-TCA GCA GTC ACA GCA GGG AAC AA-3′ for rat ENT1 (GenBank accession number NM_031684), the sense sequence was 5′-CCT ACA GCA CCC TCT TCC TCA GT-3′ and the antisense sequence was 5′-CCC AGC CAA TCC ATG ACG TTG AA-3′ for rat ENT2 (GenBank accession number NM_031738) [18], the sense sequence was 5′-CAA CAC ACA GAG GCA AAG AGA GTC-3′ and the antisense sequence was 5′-CCA CAC CAG CAG CAA GGG CTA G-3′ for rat CNT1 (GenBank accession number NM_053863), the sense sequence was 5′-GGA AGA GTG ACT TGT GCA AGC TTG-3′ and the antisense sequence was 5′-GTG CTG GTA TAG AGG TCA CAG CA-3′ for rat CNT2 (GenBank accession number NM_031664), and the sense sequence was 5′-CTG TCT TTT GGG GAA TTG GAC TGC-3′ and the antisense sequence was 5′-CCA GTA GTG GAG ACT CTG TTT GC-3′ for rat CNT3 (GenBank accession number NM_080908). The PCR products were separated by electrophoresis on an agarose gel in the presence of ethidium bromide and visualized under ultraviolet light. The molecular identity of the resultant product was confirmed by sequence analysis using a DNA sequencer (ABI PRISM 310; Applied Biosystems, Foster City, CA).

2.4. [^{3}H]Adenosine uptake by TR-iBRB2 cells

The [2,8-^{3}H]adenosine ([^{3}H]adenosine, 35.9 Ci/mmol, Amersham Life Science, Buckinghamshire, UK) uptake by TR-iBRB2 cells was measured according to a previous report [15]. Briefly, TR-iBRB2 cells (1×10^5 cells/cm^2) were cultured at 33 °C for 48 hours on rat tail collagen type I-coated 24-well plates (BD Biosciences) and washed with 1 mL extracellular fluid (ECF) buffer consisting of 122 mM NaCl, 25 mM $NaHCO_3$, 3 mM KCl, 1.4 mM $CaCl_2$, 1.2 mM $MgSO_4$, 0.4 mM K_2HPO_4, 10 mM D-glucose and 10 mM HEPES (pH 7.4) at 37 °C. Uptake was initiated by applying 200 μL ECF buffer containing 0.1 μCi [^{3}H]adenosine (14 nM) at 37 °C in the presence or absence of inhibitors. Na^+-free ECF buffers were prepared by equimolar replacement of NaCl and $NaHCO_3$ with choline chloride and choline bicarbonate, respectively. After a predetermined period, uptake was terminated by removing the solution, and cells were immersed in ice-cold ECF buffer. The cells were then solubilized in 1 N NaOH and subsequently neutralized. An aliquot was taken for measurement of radioactivity and protein content using, respectively, a liquid scintillation counter (LS6500; Beckman-Coulter, Fullerton, CA) and a DC protein assay kit (Bio-rad, Hercules, CA) with bovine serum albumin as a standard.

For kinetic studies, the Michaelis–Menten constant (K_m) and maximum rate (J_{max}) of adenosine uptake were calculated from the following equation using the nonlinear least-square regression analysis program, MULTI [19].

$$J = J_{max} \times [S]/(K_m + [S]) \quad (1)$$

where $[S]$ and J are, respectively, the concentration of adenosine and the carrier-mediated component of the uptake rate of adenosine at 5 min estimated by subtracting the uptake rate in the presence of 10 mM non-radiolabeled adenosine, which represents a non-saturable component of the uptake rate.

2.5. Quantitative real-time PCR

Quantitative real-time PCR was performed using an ABI PRISM 7700 sequence detector system (Applied Biosystems) with 2× SYBR Green PCR Master Mix (Applied Biosystems) according to the manufacturer's protocol. To quantify the amount of specific mRNA in the samples, a standard curve was generated for each run using the plasmid (pGEM-T Easy Vector; Promega, Madison, WI) containing the gene of interest. This enabled standardization of the initial mRNA content of cells relative to the amount of β-actin. The PCR was performed using ENT1, ENT2, or β-actin-specific primers and the cycling parameters are those given above. The sequences of the specific primers of rat β-actin (GenBank accession number NM_031144) were as follows: sense, 5′-TCA TGA AGT GTG ACG TTG ACA TCC GT-3′ and antisense, 5′-CCT AGA AGC ATT TGC GGT GCA CGA TG-3′.

2.6. Blood-to-retina [^{3}H]adenosine transport studies

The apparent retinal uptake clearance of [^{3}H]adenosine ($K_{in,\ retina}$) [μL/(min g retina)] from the circulating blood to the retina was determined by integration plot analysis as described previously [15]. Briefly, the rats were anesthetized with an intramuscular injection of ketamine-xylazine (1.22 mg xylazine and 125 mg ketamine/kg) and then [^{3}H]adenosine (12 μCi/head) was injected into the femoral vein. After collection of blood samples, rats were decapitated, and the retinas were removed. The retinas were dissolved in 2 N NaOH and subsequently neutralized. The radioactivity was measured in a liquid scintillation counter. As an index of the retinal distribution characteristics of [^{3}H]adenosine, the apparent retina-to-plasma concentration ratio (V_d) was used. This ratio [$V_d(t)$] (mL/g retina) was defined as the amount of [^{3}H] per gram retina divided by that per milliliter plasma, calculated over the time-period of the experiment (t). The apparent blood-to-plasma concentration ratio (R_B) was also measured to examine the [^{3}H]adenosine uptake into the blood cells. The $K_{in,\ retina}$ can be described by following Eq. (2):

$$V_d(t) = K_{in.\ retina} \times AUC(t)/C_p(t) + V_i \quad (2)$$

where AUC(t) (dpm min/mL), $C_p(t)$ (dpm/mL), and V_i (mL/g retina) represent the area under the plasma concentration time curve of [^{3}H]adenosine from time 0 to t, the plasma [^{3}H]adenosine concentration at time t, and the rapidly equilibrated distribution volume of [^{3}H]adenosine in the retina, respectively. V_i is usually comparable with the vascular volume of the retina.

The inhibitory effect of nucleosides on the blood-to-retina transport of [^{3}H] adenosine was evaluated by the retinal uptake index (RUI) method [20,21]. Briefly, the rats were anesthetized with an intramuscular injection of ketamine-xylazine and then 200 μL of injection solution was injected into the common carotid artery. The injection solution consisted of Ringer–HEPES buffer (141 mM NaCl, 4 mM KCl, 2.8 mM $CaCl_2$, 10 mM HEPES, pH 7.4) which contained both a test compound, 10 μCi [^{3}H]adenosine or D-[1-^{3}H(N)]mannitol ([^{3}H]D-mannitol, 17 Ci/mmol, PerkinElmer Life Sciences, Boston, MA), and a reference compound, 0.1 μCi n-[1-^{14}C]butanol ([^{14}C]n-butanol, 2 mCi/mmol, American Radiolabeled Chemicals, St. Louis, MO), in the presence or absence of inhibitors. Rats were decapitated at 15 sec after injection, and the retina was removed. The retina was dissolved in 2 N NaOH and subsequently neutralized. The radioactivity was measured in a liquid scintillation counter. In this study, the RUI value was used as an index of the retinal distribution characteristics of [^{3}H] adenosine and can be described by following Eq. (3):

$$RUI = \frac{[^3H]/[^{14}C](\text{dpm in the retina})}{[^3H]/[^{14}C](\text{dpm in the injection solution})} \times 100 \quad (3)$$

2.7. Data analysis

Unless otherwise indicated, all data represent means±S.E.M. An unpaired, two-tailed Student's t-test was used to determine the significance of differences between two groups. Statistical significance of differences among means of several groups was determined by one-way analysis of variance followed by the modified Fisher's least-squares difference method.

3. Results

3.1. Expression of nucleoside transporters in TR-iBRB2 cells

RT-PCR analysis was performed to examine the expression of ENT and CNT mRNAs in the rat retina and TR-iBRB2 cells. As shown in Fig. 1, the expression of ENT1, ENT2, CNT1, and CNT2 in the retina was detected at 431, 562, 479, and 298 bp, respectively. Of the four transporters, the expression of ENT1, ENT2, and CNT2 was also detected in TR-iBRB2 cells. The expression of CNT3 was not detected in the retina, however, and only a minor band of CNT3 was detected in TR-iBRB2 cells.

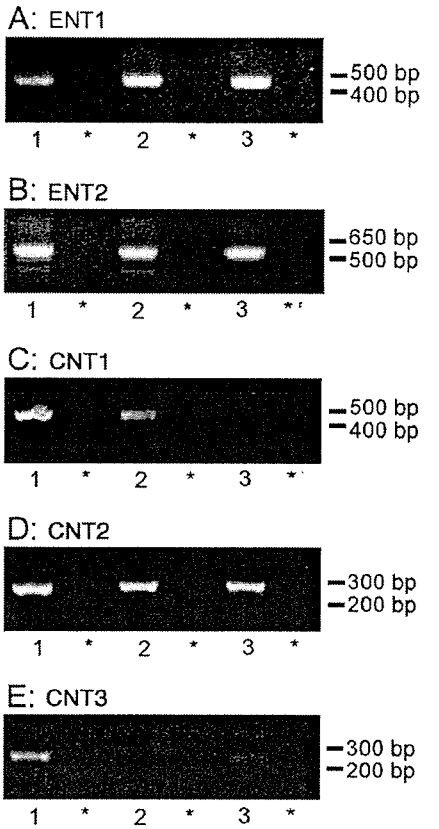

Fig. 1. RT-PCR analysis of ENT1 (A), ENT2 (B), CNT1 (C), CNT2 (D), and CNT3 (E) expression in TR-iBRB2 cells. Lane 1: positive control; lane 2: rat retina; lane 3: TR-iBRB2 cells. *: in the absence of reverse transcriptase for the respective left-hand lane. Rat brain (ENT1 and ENT2), kidney (CNT1), liver (CNT2), and small intestine (CNT3) were used as positive controls.

3.2. [^{3}H]Adenosine uptake by TR-iBRB2 cells

To analyze the kinetics and characteristics of adenosine transport at the inner BRB, [^{3}H]adenosine uptake was investigated using TR-iBRB2 cells as an in vitro model of the inner BRB. The time-courses of [^{3}H]adenosine uptake by TR-iBRB2 cells in the presence or absence of Na^+ are shown in Fig. 2. [^{3}H]Adenosine uptake increased linearly for at least 10 min. Na^+-free conditions had no effect on [^{3}H]adenosine uptake until 10 min, supporting the hypothesis that [^{3}H] adenosine uptake by TR-iBRB2 cells is predominantly mediated by ENT.

Fig. 3 shows the concentration-dependent uptake of adenosine by TR-iBRB2 cells. The Eadie–Scatchard plot (Fig. 3, inset) gave a single straight line, indicating that one saturable process was involved in adenosine uptake by TR-iBRB2 cells. Kinetic analysis of the uptake data using Eq. (1) and nonlinear least-squares regression analysis, gave a K_m of 28.5±2.2 μM and a J_{max} of 814±45 pmol/(min mg protein) (mean±S.D.).

The inhibition study was performed to characterize the [^{3}H] adenosine transport system in TR-iBRB2 cells (Table 1). Of the nucleosides studied, adenosine, inosine, uridine, and thymidine,

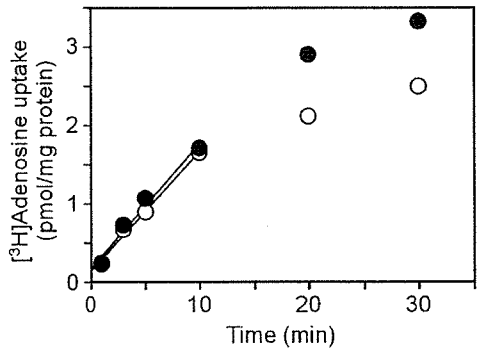

Fig. 2. Time-course of [^{3}H]adenosine uptake by TR-iBRB2 cells. The [^{3}H] adenosine (14 nM) uptake was performed at 37 °C in the presence (closed circle) or absence (open circle) of Na^+. Each point represents the mean±S.E.M. (n=4). The error bar is smaller than the size of the symbol.

at a concentration of 2 mM, inhibited [^{3}H]adenosine uptake by more than 60%, while guanosine and cytidine, at a concentration of 2 mM, partially inhibited it by up to 40%. [^{3}H] Adenosine uptake was also inhibited by nucleobases, such as 2 mM adenine and 2 mM hypoxanthine, by 41% and 28%, respectively. The Na^+-independent nucleoside transport systems can be classified according to their sensitivity to NBMPR and dipyridamole [8]. NBMPR and dipyridamole, at a concentration of 100 nM, did not inhibit [^{3}H]adenosine uptake, while NBMPR (10 and 100 μM) and dipyridamole (1 and 10 μM) produced more than 50% inhibition. These results represent NBMPR- and dipyridamole-insensitive transport of adenosine in TR-iBRB2 cells.

3.3. Expression levels of ENT1 and ENT2 in TR-iBRB2 cells

To determine the dominant ENT in TR-iBRB2 cells, quantitative real-time PCR analysis was performed to quantify the mRNA expression levels of ENT1 and ENT2 in TR-iBRB2 cells (Fig. 4). The degree of mRNA expression compensated with β-actin, for ENT1 and ENT2 was $3.27\pm0.29\times10^{-3}$ and $1.81\pm0.33\times10^{-2}$, respectively. Accordingly, the expression of ENT2 mRNA was 5.5-fold greater than that of ENT1 in TR-iBRB2 cells.

Table 1
Effect of several inhibitors on [^{3}H]adenosine uptake by TR-iBRB2 cells

	Inhibitors	Percentage of control
	Control	100±1
2 mM	Adenosine	4.75±0.13**
2 mM	Inosine	20.9±0.3**
2 mM	Uridine	35.7±1.5**
2 mM	Thymidine	24.4±0.6**
2 mM	Guanosine	60.3±1.7**
2 mM	Cytidine	70.5±3.4**
2 mM	Adenine	59.2±4.4**
2 mM	Hypoxanthine	71.8±3.8**
100 nM	Nitrobenzylmercaptopurine riboside (NBMPR)	86.3±1.9*
10 μM	NBMPR	43.9±1.8**
100 μM	NBMPR	10.5±0.6**
100 nM	Dipyridamole	92.0±1.4
1 μM	Dipyridamole	42.3±1.7**
10 μM	Dipyridamole	8.14±0.16**

[^{3}H]Adenosine uptake (14 nM) was performed in the absence (control) or presence of 2 mM inhibitors at 5 min and 37 °C. Each value represents the mean±S.E.M. (n=4–12).
* $P<0.05$ significantly different from the control.
** $P<0.001$, significantly different from the control.

3.4. Blood-to-retina transport of [^{3}H]adenosine

The in vivo blood-to-retina influx transport of adenosine from the circulating blood to the retina through the BRB was evaluated by an integration plot analysis after intravenous administration of [^{3}H]adenosine and application of the RUI method using rats. The $K_{in,\ retina}$ of [^{3}H]adenosine was found to be 25.8±0.7 μL/(min g retina) (mean±S.D.) from the slope of the integration plot (Fig. 5A). The $K_{in,\ retina}$ includes

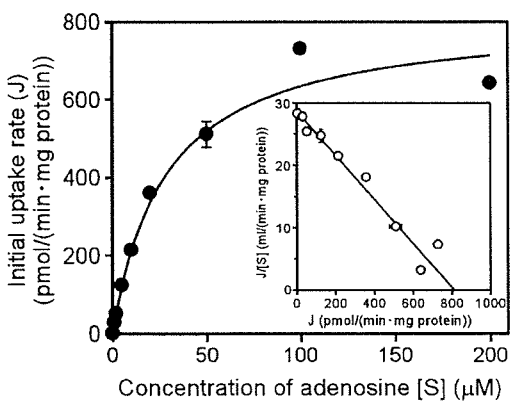

Fig. 3. Concentration-dependence of adenosine uptake by TR-iBRB2 cells. The [^{3}H]adenosine (14 nM) uptake was performed at 5 min and 37 °C. Each point represents the mean±S.E.M. (n=4). Data were subjected to Michaelis–Menten and Eadie–Scatchard analyses (inset). The K_m is 28.5±2.2 μM and J_{max} is 814±45 pmol/(min mg protein) (mean±S.D.).

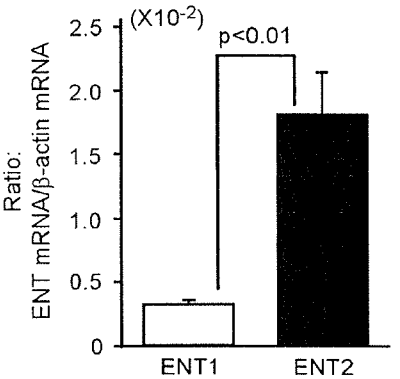

Fig. 4. The amount of ENT1 and ENT2 mRNA in TR-iBRB2 cells. The amount of ENT1 and ENT2 mRNA in TR-iBRB2 cells was determined by quantitative real-time PCR analysis. Data are the mean±S.E.M. (n=4). The quantity of ENT1 mRNA relative to β-actin mRNA (ENT1/β-actin) in TR-iBRB2 cells was $3.27\pm0.29\times10^{-3}$, and that of ENT2 mRNA (ENT2/β-actin) was $1.81\pm0.33\times10^{-2}$.

the apparent uptake clearance into the retinal blood (e.g. erythrocytes) as well as the apparent influx clearance across the BRB. In the case of adenosine, the apparent uptake clearance into the retinal blood cannot be ignored, since the R_B of [^{3}H]adenosine was increased with a slope of 0.0882 ± 0.0149 min^{-1} (mean±S.D.) (Fig. 5B). This behavior of adenosine is consistent with a previous report showing that adenosine accumulates in erythrocytes [22]. The vascular volume in the retina was found to be 0.167±0.010 mL/g retina from the V_i of [^{3}H]adenosine (Fig. 5A). By multiplying the slope of the R_B increment and the vascular volume in the retina, the apparent uptake clearance into retinal blood found to be 14.7±3.3 μL/(min g retina). Therefore, the apparent influx clearance across the BRB was found to be 11.1±4.1 μL/(min g retina). The influx transport of adenosine across the BRB was also supported by the fact that the estimated RUI value of [^{3}H]adenosine was greater than that of [^{3}H]D-mannitol (Table 2). Moreover, adenosine and thymidine at a concentration of 2 mM significantly decreased the RUI value of [^{3}H]adenosine to 70% and 75%, respectively, while 2 mM cytidine had no effect. These results confirm the carrier-mediated transport of adenosine from the blood to the retina across the BRB.

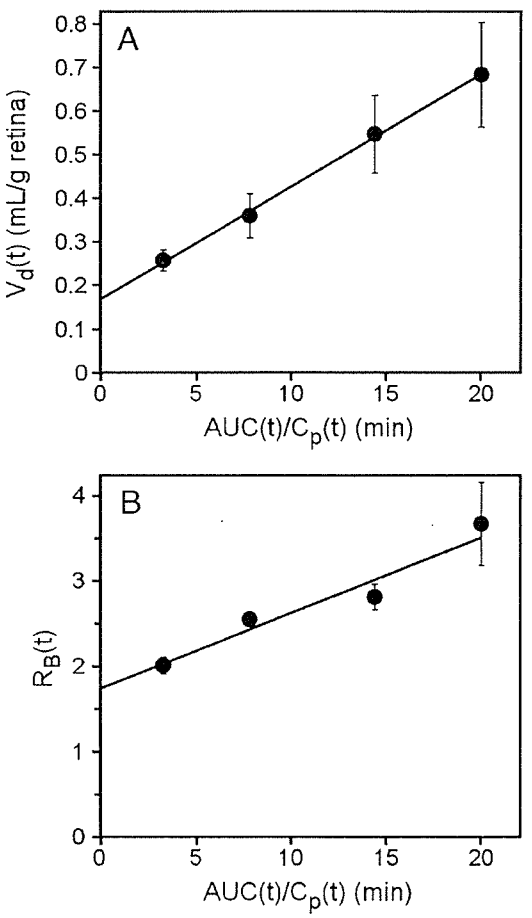

Fig. 5. Integration plot of the initial uptake of [^{3}H]adenosine by the retina (A) and blood-to-plasma concentration ratio (R_B) (B) after intravenous administration. [^{3}H]Adenosine (12 μCi/head) was injected into the femoral vein. Each point represents the mean±S.E.M. (n=3–4).

Table 2
Retinal uptake index (RUI) of [^{3}H]adenosine and [^{3}H]D-mannitol

Compounds	Inhibitors	RUI (%)	Percentage of control
[^{3}H]Adenosine		32.3±2.8	100±9
	Adenosine	22.7±3.2*	70.4±10.0*
	Thymidine	24.1±2.4*	74.7±7.3*
	Cytidine	35.0±1.7	108±5
[^{3}H]D-Mannitol		11.6±1.4	

A test compound, [^{3}H]adenosine or [^{3}H]D-mannitol (10 μCi/head), and a reference compound, [^{14}C]n-butanol (0.1 μCi/head), were injected into the common carotid artery in the presence or absence of 2 mM inhibitors. Each value represents the mean±S.E.M. (n=3–9).
* P<0.05 significantly different from the control.

4. Discussion

The present study shows that the BRB is able to transport [^{3}H]adenosine (Fig. 5). The nucleoside transporters are classified as an Na^+-independent ENT and an Na^+-dependent CNT. TR-iBRB2 cells, an in vitro model of the rat inner BRB, express both ENT and CNT mRNAs (Fig. 1), however, Na^+-independent uptake of [^{3}H]adenosine by TR-iBRB2 cells (Fig. 2) suggests that ENT is predominantly involved in the adenosine transport in TR-iBRB2 cells.

ENTs can be further sub-divided into two isoforms according to their sensitivity to NBMPR [8]. The NBMPR-sensitive (*es*) transporter, ENT1, is blocked by less than 100 nM NBMPR (IC_{50}=4.6 nM) [23] while the NBMPR-insensitive (*ei*) transporter, ENT2, requires more than 1 μM NBMPR to inhibit nucleoside transport [23]. Although both ENT1 and ENT2 have a variety of nucleoside substrates, ENT2 exhibits a lower affinity for guanosine and cytidine than ENT1 [24]. Moreover, only ENT2 is capable of low affinity transport of nucleobases, such as adenine and hypoxanthine [25]. In TR-iBRB2 cells, [^{3}H]adenosine uptake was not inhibited by NBMPR at 100 nM, but was inhibited at 10 and 100 μM (Table 1). [^{3}H]Adenosine uptake by TR-iBRB2 cells was inhibited by nucleosides, however, the degree of inhibition by adenosine, inosine, uridine, and thymidine was greater than that produced by guanosine and cytidine. In addition to nucleosides, [^{3}H]adenosine uptake by TR-iBRB2 cells was partly inhibited by nucleobases, such as adenine and hypoxanthine. Such forms of inhibition in TR-iBRB2 cells are consistent with ENT2 rather than ENT1. Moreover, quantitative real-time PCR analysis clearly demonstrated that ENT2 is predominantly expressed in TR-iBRB2 cells (Fig. 4). In the light of these findings, adenosine transport in TR-iBRB2 cells is most likely mediated by ENT2.

[^{3}H]Adenosine uptake by TR-iBRB2 cells was not inhibited by dipyridamole at 100 nM, but was inhibited at 1 and 10 μM (Table 1). Dipyridamole is also known to be a useful inhibitor for distinguishing human ENT1 from ENT2, since it blocks human ENT1 and ENT2 with a K_i of 5 nM and 360 nM, respectively [24]. However, in the rat, there are some contradictory reports about the ability of dipyridamole to inhibit rat ENT-mediated transport. The inhibitory effect

observed in human ENT is similar to that in rat C6 glioma cells [26] and rat brain microvascular endothelial cells [27,28] as well as the TR-iBRB2 cells in this study, while 1 μM dipyridamole had no effect on transport activity in recombinant rat ENT1 and ENT2 expressed in *Xenopus* oocytes [23]. These observations indicate that dipyridamole is an effective inhibitor of ENT2-mediated transport in the case of TR-iBRB2 cells, although its inhibitory effect seems to depend on the cell type and preparation used.

[^{3}H]Adenosine is transported from the circulating blood to the retina across the BRB with an apparent influx clearance of 11.1±4.1 μL/(min g retina) (Fig. 5). This value is far greater than that of [^{14}C]sucrose [0.26 μL/(min g retina)] and [^{3}H]D-mannitol [0.75 μL/(min g retina)] used as non-permeable paracellular markers [29]. The RUI value of [^{3}H]adenosine was also greater than that of [^{3}H]D-mannitol (Table 2). These results suggest that adenosine is transported via a carrier-mediated transport process, rather than by passive diffusion. Moreover, [^{3}H]adenosine uptake into the retina was inhibited by adenosine and thymidine, but was unaffected by cytidine (Table 2). These inhibitory characteristics are comparable with those obtained in TR-iBRB2 cells (Table 1). The BRB is composed of retinal capillary endothelial cells (inner BRB) and retinal pigment epithelial cells (outer BRB). In addition to TR-iBRB2 cells (Fig. 2), carrier-mediated adenosine transport has also been demonstrated in ARPE-19 cells, an in vitro model of the human outer BRB [30]. Accordingly, both the inner and outer BRB seem to be involved in [^{3}H]adenosine transport from the circulating blood to the retina. The net flux of adenosine transport at the BRB is still uncertain at the present time, since it is technically impossible to estimate the efflux clearance across the BRB. In the case of the blood–brain barrier (BBB), the efflux clearance of adenosine across the BBB is 3-fold greater than the influx clearance [31]. The adenosine concentration in the rat retina/choroid [32] (approximately 0.9 nmol/g ≈ 0.9 μM) is about 10-fold greater than that in the blood (90 nM) [31]. Since the K_m of adenosine uptake by TR-iBRB2 cells (28.5 μM; Fig. 3) is greater than the adenosine concentration in the retina/choroid as well as the blood, the transport velocity of adenosine at the inner BRB is expected to be relative to the adenosine concentration. Therefore, the net efflux of adenosine transport at the inner BRB may occur as at the BBB [31], since ENT2 is a bi-directional equilibrative transporter.

In conclusion, adenosine transport at the inner BRB is most likely mediated by ENT2. Under physiological conditions, adenosine serves as the principal mechanism of inhibitory neuromodulation [33]. However, the adenosine concentration is dramatically increased by more than 10-fold in the ischemic retina [32] and then adenosine exacerbates the effects of retinal ischemia/reperfusion and promotes retinal neovascularization [2,34]. Therefore, the possible physiological role for ENT2 at the inner BRB involves maintaining a constant milieu of adenosine in the retinal interstitial fluid especially under some pathological conditions like ischemia. The current findings represent an important contribution to our understanding of the physiological roles of the inner BRB in regulating the adenosine concentration in the retina.

Acknowledgements

The authors would like to thank Dr. Kazunori Katayama (University of Toyama) and Yoshiharu Deguchi (Teikyo University) for valuable discussions. This study was supported, in part, by a Grant-in-Aid for Scientific Research from the Japan Society for the Promotion of Science and a grant for Research on Sensory and Communicative Disorders by the Ministry of Health, Labor, and Welfare, Japan.

References

[1] G.A. Lutty, D.S. McLeod, Retinal vascular development and oxygen-induced retinopathy: a role for adenosine, Prog. Retin. Eye Res. 22 (2003) 95–111.
[2] G.J. Ghiardi, J.M. Gidday, S. Roth, The purine nucleoside adenosine in retinal ischemia–reperfusion injury, Vis. Res. 39 (1999) 2519–2535.
[3] G.W. Kreutzberg, S.T. Hussain, Cytochemical heterogeneity of the glial plasma membrane: 5′-nucleotidase in retinal Müller cells, J. Neurocytol. 11 (1982) 53–64.
[4] G.A. Lutty, C. Merges, D.S. McLeod, 5′ nucleotidase and adenosine during retinal vasculogenesis and oxygen-induced retinopathy, Investig. Ophthalmol. Vis. Sci. 41 (2000) 218–229.
[5] L. Sosula, P. Beaumont, K.M. Jonson, F.C. Hollows, Quantitative ultrastructure of capillaries in the rat retina, Invest. Ophthalmol. 11 (1972) 916–925.
[6] K. Hosoya, M. Tomi, Advances in the cell biology of transport via the inner blood–retinal barrier: establishment of cell lines and transport functions, Biol. Pharm. Bull. 28 (2005) 1–8.
[7] E. Polska, P. Ehrlich, A. Luksch, G. Fuchsjager-Mayrl, L. Schmetterer, Effects of adenosine on intraocular pressure, optic nerve head blood flow, and choroidal blood flow in healthy humans, Investig. Ophthalmol. Vis. Sci. 44 (2003) 3110–3114.
[8] S.A. Baldwin, P.R. Beal, S.Y. Yao, A.E. King, C.E. Cass, J.D. Young, The equilibrative nucleoside transporter family, SLC29, Pflugers Arch. 447 (2004) 735–743.
[9] J.H. Gray, R.P. Owen, K.M. Giacomini, The concentrative nucleoside transporter family, SLC28, Pflugers Arch. 447 (2004) 728–734.
[10] M.A. Ackley, R.J. Governo, C.E. Cass, J.D. Young, S.A. Baldwin, A.E. King, Control of glutamatergic neurotransmission in the rat spinal dorsal horn by the nucleoside transporter ENT1, J. Physiol. 548 (2003) 507–517.
[11] B.J. Meester, N.P. Shankley, N.J. Welsh, F.L. Meijler, J.W. Black, Pharmacological analysis of the activity of the adenosine uptake inhibitor, dipyridamole, on the sinoatrial and atrioventricular nodes of the guinea-pig, Br. J. Pharmacol. 124 (1998) 729–741.
[12] C. Blazynski, The accumulation of [^{3}H]phenylisopropyl adenosine ([3H] PIA) and [^{3}H]adenosine into rabbit retinal neurons is inhibited by nitrobenzylthioinosine (NBI), Neurosci. Lett. 121 (1991) 1–4.
[13] R. Paes de Carvalho, K.M. Braas, S.H. Snyder, R. Adler, Analysis of adenosine immunoreactivity, uptake, and release in purified cultures of developing chick embryo retinal neurons and photoreceptors, J. Neurochem. 55 (1990) 1603–1611.
[14] K. Hosoya, M. Tomi, S. Ohtsuki, H. Takanaga, M. Ueda, N. Yanai, M. Obinata, T. Terasaki, Conditionally immortalized retinal capillary endothelial cell lines (TR-iBRB) expressing differentiated endothelial cell functions derived from a transgenic rat, Exp. Eye Res. 72 (2001) 163–172.
[15] K. Hosoya, A. Minamizono, K. Katayama, T. Terasaki, M. Tomi, Vitamin C transport in oxidized form across the rat blood–retinal barrier, Investig. Ophthalmol. Vis. Sci. 45 (2004) 1232–1239.
[16] T. Nakashima, M. Tomi, K. Katayama, M. Tachikawa, M. Watanabe, T. Terasaki, K. Hosoya, Blood-to-retina transport of creatine via creatine transporter (CRT) at the rat inner blood–retinal barrier, J. Neurochem. 89 (2004) 1454–1461.
[17] M. Tomi, M. Mori, M. Tachikawa, K. Katayama, T. Terasaki, K. Hosoya, L-Type amino acid transporter 1 (LAT1)-mediated L-leucine transport at

the inner blood–retinal barrier, Investig. Ophthalmol. Vis. Sci. 46 (2005) 2522–2530.
[18] T. Kitano, H. Iizasa, T. Terasaki, T. Asashima, N. Matsunaga, N. Utoguchi, Y. Watanabe, M. Obinata, M. Ueda, E. Nakashima, Polarized glucose transporters and mRNA expression properties in newly developed rat syncytiotrophoblast cell lines, TR-TBTs, J. Cell. Physiol. 193 (2002) 208–218.
[19] K. Yamaoka, Y. Tanigawara, T. Nakagawa, T. Uno, A pharmacokinetic analysis program (multi) for microcomputer, J. Pharmacobio-dyn. 4 (1981) 879–885.
[20] Y.S. Kang, T. Terasaki, A. Tsuji, Acidic drug transport in vivo through the blood–brain barrier. A role of the transport carrier for monocarboxylic acids, J. Pharmacobio-dyn. 13 (1990) 158–163.
[21] A. Alm, P. Törnquist, The uptake index method applied to studies on the blood–retinal barrier. I. A methodological study, Acta Physiol. Scand. 113 (1981) 73–79.
[22] E. Snoeck, K. Ver Donck, P. Jacqmin, H. Van Belle, A.G. Dupont, A. Van Peer, M. Danhof, Physiological red blood cell kinetic model to explain the apparent discrepancy between adenosine breakdown inhibition and nucleoside transporter occupancy of draflazine, J. Pharmacol. Exp. Ther. 286 (1998) 142–149.
[23] S.Y. Yao, A.M. Ng, W.R. Muzyka, M. Griffiths, C.E. Cass, S.A. Baldwin, J.D. Young, Molecular cloning and functional characterization of nitrobenzylthioinosine (NBMPR)-sensitive (es) and NBMPR-insensitive (ei) equilibrative nucleoside transporter proteins (rENT1 and rENT2) from rat tissues, J. Biol. Chem. 272 (1997) 28423–28430.
[24] J.L. Ward, A. Sherali, Z.P. Mo, C.M. Tse, Kinetic and pharmacological properties of cloned human equilibrative nucleoside transporters, ENT1 and ENT2, stably expressed in nucleoside transporter-deficient PK15 cells. ENT2 exhibits a low affinity for guanosine and cytidine but a high affinity for inosine, J. Biol. Chem. 275 (2000) 8375–8381.
[25] S.Y. Yao, A.M. Ng, M.F. Vickers, M. Sundaram, C.E. Cass, S.A. Baldwin, J.D. Young, Functional and molecular characterization of nucleobase transport by recombinant human and rat equilibrative nucleoside transporters 1 and 2. Chimeric constructs reveal a role for the ENT2 helix 5–6 region in nucleobase translocation, J. Biol. Chem. 277 (2002) 24938–24948.
[26] C.J. Sinclair, C.G. LaRiviere, J.D. Young, C.E. Cass, S.A. Baldwin, F. E. Parkinson, Purine uptake and release in rat C6 glioma cells: nucleoside transport and purine metabolism under ATP-depleting conditions, J. Neurochem. 75 (2000) 1528–1538.
[27] M. Chishty, D.J. Begley, N.J. Abbott, A. Reichel, Functional characterisation of nucleoside transport in rat brain endothelial cells, NeuroReport 14 (2003) 1087–1090.
[28] F.E. Parkinson, J. Friesen, L. Krizanac-Bengez, D. Janigro, Use of a three-dimensional in vitro model of the rat blood–brain barrier to assay nucleoside efflux from brain, Brain Res. 980 (2003) 233–241.
[29] S.L. Lightman, A.G. Palestine, S.I. Rapoport, E. Rechthand, Quantitative assessment of the permeability of the rat blood–retinal barrier to small water-soluble non-electrolytes, J. Physiol. 389 (1987) 483–490.
[30] S. Majumdar, S. Macha, D. Pal, A.K. Mitra, Mechanism of ganciclovir uptake by rabbit retina and human retinal pigmented epithelium cell line ARPE-19, Curr. Eye Res. 29 (2004) 127–136.
[31] A.J. Isakovic, N.J. Abbott, Z.B. Redzic, Brain to blood efflux transport of adenosine: blood–brain barrier studies in the rat, J. Neurochem. 90 (2004) 272–286.
[32] S. Roth, P.S. Rosenbaum, J. Osinski, S.S. Park, A.Y. Toledano, B. Li, A.A. Moshfeghi, Ischemia induces significant changes in purine nucleoside concentration in the retina-choroid in rats, Exp. Eye Res. 65 (1997) 771–779.
[33] E.A. Newman, Glial cell inhibition of neurons by release of ATP, J. Neurosci. 23 (2003) 1659–1666.
[34] R.P. Mino, P.E. Spoerri, S. Caballero, D. Player, L. Belardinelli, I. Biaggioni, M.B. Grant, Adenosine receptor antagonists and retinal neovascularization in vivo, Investig. Ophthalmol. Vis. Sci. 42 (2001) 3320–3324.

ELSEVIER

Journal of Neuroscience Methods 156 (2006) 249–256

JOURNAL OF NEUROSCIENCE METHODS

www.elsevier.com/locate/jneumeth

Application of microdialysis to evaluate the efflux transport of estradiol 17-β glucuronide across the rat blood–retinal barrier

Kazunori Katayama, Yuki Ohshima, Masatoshi Tomi, Ken-ichi Hosoya *

Department of Pharmaceutics, Graduate School of Medical and Pharmaceutical Sciences, University of Toyama, 2630 Sugitani, Toyama 930-0194, Japan

Received 9 February 2006; received in revised form 9 March 2006; accepted 14 March 2006

Abstract

The purpose of the present study was to evaluate vitreous humor/retina-to-blood efflux transport in rats and determine the efflux transport of estradiol 17-β glucuronide (E17βG) across the blood–retinal barrier (BRB) by the use of microdialysis. [^{3}H]E17βG and [^{14}C]D-mannitol, which were used as a model compound for amphipathic organic anions and a bulk flow marker, respectively, were injected into the vitreous humor of rat eye, and a microdialysis probe was placed in the vitreous humor. [^{3}H]E17βG and [^{14}C]D-mannitol were bi-exponentially eliminated from the vitreous humor after vitreous bolus injection. The elimination rate constant of [^{3}H]E17βG during the terminal phase was 1.9-fold greater than that of [^{14}C]D-mannitol and reduced the level of [^{14}C]D-mannitol in the retinal presence of 0.3 mM E17βG, suggesting that [^{3}H]E17βG is transported via a carrier-mediated efflux transport process across the BRB. The efflux transport of [^{3}H]E17βG was significantly inhibited by organic anions, such as probenecid, sulfobromophthalein, digoxin, and dehydroepiandrosterone sulfate, whereas it was not inhibited by *p*-aminohippuric acid. In conclusion, the efflux transport of [^{3}H]E17βG across the rat BRB was evaluated by microdialysis and its inhibition by organic anions suggests organic anion transporting polypeptide 1a4-mediated E17βG efflux transport at the BRB.

Keywords: Blood–retinal barrier; Microdialysis; Organic anion; Organic anion transporting polypeptide (Oatp)1a4; Efflux transport

1. Introduction

The blood–retinal barrier (BRB), which forms complex tight junctions of retinal capillary endothelial cells (inner BRB) and retinal pigment epithelial cells (RPE; outer BRB), maintains a constant milieu and shields the neural retina from the circulating blood (Cunha-Vaz, 2004; Hosoya and Tomi, 2005). In addition to the structural barrier, the inner BRB expresses P-glycoprotein, which appears to restrict the blood-to-retina transport of hydrophobic drugs, such as cyclosporin A and quinidine (BenEzra and Maftzir, 1990; Duvvuri et al., 2003; Hosoya and Tomi, 2005). It is important to characterize influx and efflux transport processes at the BRB for drug distribution to the retina since the pharmacological effects of the drug in that tissue are governed by the retinal drug concentration. The blood-to-retina influx transport of the substrates has been investigated using the retinal uptake index method (Alm and Törnquist, 1981) and in vivo integration plot analysis (Hosoya et al., 2004), but it is limited to an evaluation of the retina-to-blood efflux transport of the substrates. It is important to elucidate the retina-to-blood efflux transport processes for organic anions since drugs, hormones, and neurotransmitters are mostly metabolized in the form of organic anions in the retina and need to undergo efflux transport from the retina to the blood across the BRB.

Vitreous fluorophotometry has been used to determine the transport of fluorescein, an organic anion, across the BRB in the blood-to-vitreous humor direction as well as in the opposite direction (Cunha-Vaz and Maurice, 1969; Engler et al., 1994). Engler et al. (1994) found that the fluorescein transport in the vitreous humor-to-blood direction is more than 100-fold greater than that in the opposite direction and is inhibited in the presence of probenecid, suggesting that fluorescein transported across the BRB is involved in the carrier-mediated organic anion transport process. Although this method is very useful for monitoring the integrity of the BRB, it is of limited value for studying the efflux transport of other organic anions since it is necessary to use a fluorescent probe.

Microdialysis has been recognized as a valuable tool for sampling the extracellular space of living tissue (Deguchi and Morimoto, 2001; Tunblad et al., 2004). This has been applied to

* Corresponding author. Tel.: +81 76 434 7505; fax: +81 76 434 5172.
E-mail address: hosoyak@pha.u-toyama.ac.jp (K.-i. Hosoya).

0165-0270/$ – see front matter © 2006 Elsevier B.V. All rights reserved.
doi:10.1016/j.jneumeth.2006.03.012

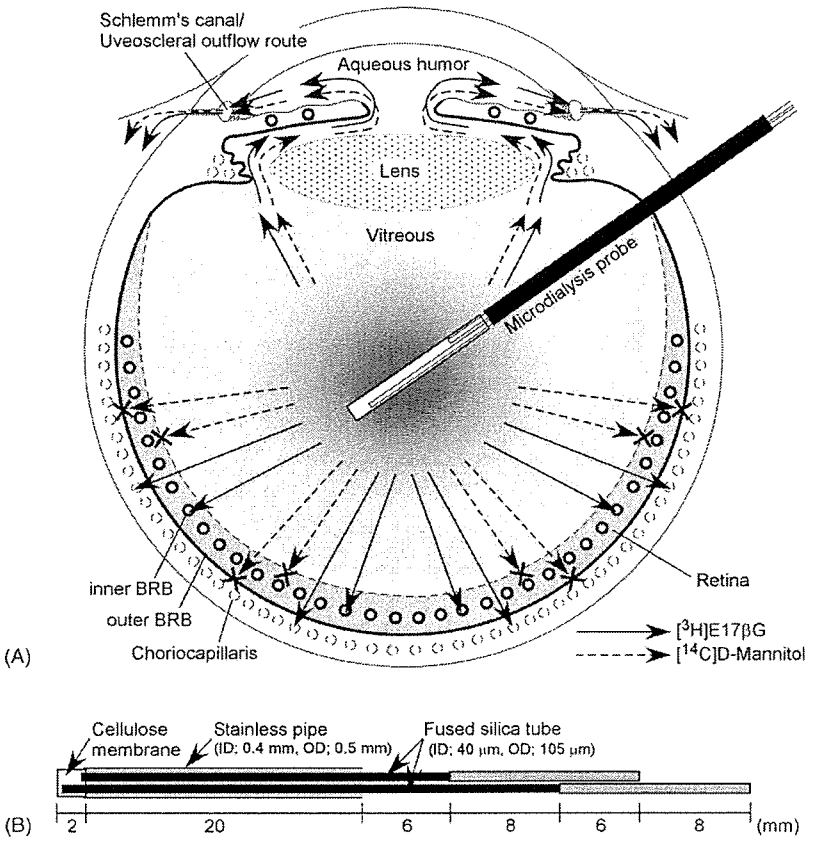

Fig. 1. Diagrammatic representation of the routes of elimination of [^{3}H]E17βG and [^{14}C]D-mannitol after vitreous bolus injection (A) and microdialysis probe (B). The microdialysis probe is implanted after vitreous bolus injection of both [^{3}H]E17βG and [^{14}C]D-mannitol. Bold and dashed lines represent the tight epithelial barrier and porous tissue boundary, respectively. Bold and dashed circles represent tight and fenestrated blood vessels, respectively (A). The custom-designed microdialysis probe (TEP-50) was constructed by Eicom (Kyoto, Japan) (B).

sampling vitreous fluid in the rabbit and monitoring drug concentrations in the vitreous humor (Anand et al., 2004; Macha and Mitra, 2001) and neurotransmitter concentrations in vitreous/retina tissue (Louzada-Junior et al., 1992). Macha and Mitra (2001) have reported the intravitreal kinetics of fluorescein after intravitreal administration using two microdialysis probes implanted in the anterior and vitreous chambers of the rabbit eye. The vitreous concentration of fluorescein decayed bi-exponentially and fluorescein appeared in the aqueous humor, suggesting that fluorescein is eliminated from the anterior chamber via Schlemm's canal and/or the uveoscleral outflow route as well as via the BRB (Engler et al., 1994; Macha and Mitra, 2001; Sears, 1983) (Fig. 1A). Although rabbits are generally used to evaluate the ocular kinetics of drugs because they have a similar size of eye compared with humans (Macha and Mitra, 2001; Rittenhouse et al., 1999), the anatomy of the rabbit eye is unusual among mammals. The retinal vessels are limited to a stripe of myelinated tissue that radiates horizontally from the optic nerve head, while the remainder of the retina is avascular (Pow, 2001; Sen et al., 1992) and drug transport between retina and blood is mainly via the outer BRB. The retinas in humans and rats are well vascularized and have an inner BRB as well as an outer BRB (Pow, 2001). Therefore, it is important to evaluate the vitreous humor/retina-to-blood efflux transport of organic anions in rats. Moreover, data can be compared with previous blood-to-retinal influx transport data generated from in vivo and in vitro studies in rats (Alm and Törnquist, 1981; Hosoya et al., 2001, 2004; Lightman et al., 1987).

The purpose of the present study was to carry out an in vivo evaluation of vitreous humor/retina-to-blood efflux transport in rats and determine the efflux transport of estradiol 17-β glucuronide (E17βG) across the BRB. We used a microdialysis probe, which was designed for the rat eye, and inserted it into the rat vitreous humor. Using this approach, we estimated the efflux transport of E17βG from the vitreous humor/retina to the blood across the BRB by monitoring the concentration of [^{3}H]E17βG and [^{14}C]D-mannitol, used as a model compound for amphipathic organic anions and a bulk flow marker, respectively, in the vitreous humor (Fig. 1).

2. Materials and methods

2.1. Animals

Male Wistar rats, weighing 250–300 g, were purchased from SLC (Shizuoka, Japan). The investigations using rats described in this report conformed to the provisions of the Animal Care Committee, Toyama Medical and Pharmaceutical University